10.1109/ULTSYM.2011.0292

Characterization of Red Blood Cell Aggregation with Photoacoustics: A Theoretical and Experimental Study

Eno Hysi, Ratan K. Saha and Michael C. Kolios
Department of Physics, Ryerson University, Toronto, ON, M5B 2K3, Canada

***Abstract*-The aggregation of red blood cells (RBCs) is a phenomenon that is governed by plasma fibrinogen concentration and the shear forces of flow. We propose the use of photoacoustics (PA) for the detection and characterization of RBC aggregation. A 2D simulation study was performed to investigate the dependence of the PA signal on hematocrit for non-aggregated cells and on the aggregate size for aggregated samples. Experimental confirmation of theoretical results was conducted using human RBC samples and the Imagio PA imaging device (Seno Medical Instruments Inc., San Antonio, TX). Samples were exposed to 1064 nm laser irradiation. PA signals were collected from the non-aggregated samples at varying hematocrit levels. Aggregation was induced by suspending the RBCs in various concentrations of Dextran-70. To account for the response of the imaging system, the PA spectra were calibrated by dividing by the response of the transducer measured using a needle hydrophone. Theoretical and experimental results show a monotonic increase in the PA signal amplitude with increasing hematocrit. As the size of aggregates increases, simulations demonstrate a shift towards lower frequencies in the PA power spectrum as well as enhancements as large as 11 dB compared to the non-aggregated sample. Experimental results confirm the ability of PA to detect and quantify the aggregation of RBCs. PA radiofrequency spectral analysis seems provides a quantitative means for distinguishing between aggregated and non-aggregated samples.**

I. INTRODUCTION

Red blood cells (RBCs) have the tendency to form reversible aggregates. The RBCs form a structure frequently referred to as rouleaux and given sufficient time, individual rouleaux can cluster, forming 3D networks [1]. RBC aggregation is associated with elevated levels of plasma macromolecules such as fibrinogen and the aggregation is governed by flow shear forces [2]. Thus, the aggregation level plays an important role in blood flow, particularly in the microvascular system. It increases blood viscosity and affects the passage of cells through micro vessels, especially in venules with low shear flow [3]. Increased RBC aggregation has been associated to a variety of pathological states such as diabetes, thrombosis, myocardial infarction and sepsis [4].

In current clinical practice, all available techniques used for characterizing RBC aggregation require the invasive withdrawal of blood thus further manipulating the process of aggregation. Several in-vitro experimental techniques have been developed to assess aggregation but they either make use of ionizing radiation or are not feasible for in-vivo assessment [5], [6]. A great deal of effort has been invested into developing ultrasound (US) backscattering techniques as non-invasive tools to monitor RBC aggregation [7], [8].

In this work, we propose the use of photoacoustics (PA) for the detection and characterization of RBC aggregation. PA is a non-invasive, hybrid imaging modality which probes the optical and thermoelastic properties of tissue by detecting pressure waves produced by laser irradiation [9]. The motivation in using PA lies in the ability to combine the US resolution in the receiving end with the optical contrast provided by the large differences in the light absorption of different tissues. By taking advantage of the large oxygen dependent optical absorption of blood, PA is capable of producing oxygen saturation maps of vasculature [10]. To the best of our knowledge, PA has never been used for characterizing the level of RBC aggregation.

PA images, much like conventional US images, are typically reconstructed by displaying only the amplitude of the radiofrequency (RF) signals detected by passive US transducers. Images recorded this way depend on the US transducer response thus making the results system-dependent. In US, spectral characterization of backscattered RF signals (frequency-domain analysis) been developed for quantitative tissue characterization and therapy response monitoring [11], [12]. This approach uses the frequency response of the US transducer to calibrate the measured power spectra from a region of interest (ROI), resulting in a quasi-linear spectrum over the usable US bandwidth. Performing linear regression yields a set of parameters (slope, intercept and midband fit) which have been related to structural tissue properties such as acoustic scatter size and concentration [13]. To date, such frequency-domain analysis of PA imaging data has only been implemented for assessing prostate adenocarcinoma tumors in a murine model as well as for detecting abnormal vasculature [14], [15]. It is reasonable to expect that the PA spectra will contain information about the size and concentration of optical absorbers (i.e. RBCs).

We present a theoretical model which simulates the PA signals from non-aggregating (NA) and aggregating (AG) RBCs. It uses a frequency-domain approach to calculate the PA field generated by RBCs. PA RF spectral analysis is then used to differentiate and characterize the level of aggregation of NA and AG RBCs. Experimental verification of the model is done using human RBCs and Dextran-70 to induce aggregation. PA spectral parameters are computed for NA and AG RBCs from calibrated PA spectra.

II. Materials And Methods

A. Computer simulation

Two-dimensional blood tissue realizations were generated using the Monte Carlo method described by a recent publication by our group [16]. Coordinates of NA RBCs (modeled as spheres) were randomly chosen with the restriction that they would not overlap with existing particles under periodic boundary conditions. A hexagonal close packing scheme was used to arrange individual RBC forming an aggregate which is randomly and repeatedly placed within a ROI. The frequency domain PA pressure generated from an ensemble of absorbing spheres can be written as the linear superposition of the spherical waves emitted by the individual sources [17]:

$$p_f(q) = \frac{i\mu\beta I_0 v_s a}{C_P(r/a)} \frac{[\sin q - q\cos q]e^{ik_f(r-a)}}{q^2[(1-\rho)(\sin q/q) - \cos q + i\rho v \sin q]} \sum_{n=1}^{N} e^{-i\vec{k}_f \cdot \vec{r}_n} \quad (1)$$

where the subscripts f and s denote the fluid and sphere respectively. The dimensionless frequency q is defined as $q = \omega a/v_s$ and a is the radius of the absorbing sphere. Here, ω is the optical radiation modulation frequency. Similarly, μ is the optical absorption coefficient, β is the isobaric thermal expansion coefficient, C_P is the heat capacity per unit mass, I_0 is the intensity of the optical radiation, r_n is the position vector of the n^{th} particle, k_f is the wave number in the fluid medium, and $\rho = \rho_s/\rho_f$ and $v = v_s/v_f$ represent the ratios of sphere to fluid density and the sphere to fluid speed of sound, respectively. For each sample 250 complex PA signals were computed from 250 different configurations by taking the inverse Fourier transform of (1). The effect of hematocrit and aggregate size on the PA power spectra was investigated. The physical constants and parameters used in this simulation are shown in Table I.

TABLE I
SIMULATION PARAMETERS

ROI	$200 \times 200\ \mu m^2$
a	$2.75\ \mu m$
ρ_s	$1092\ kg/m^3$
v_s	$1639\ m/s$
ρ_f	$1005\ kg/m^3$
v_f	$1498\ m/s$
β	$1\ K^{-1}$
C_P	$1\ Jkg^{-1}K^{-1}$
μ	$1\ m^{-1}$

B. RBC preparation

Human RBCs from a single donor were purchased from Innovative Research Inc. (Novi, MI, USA). The cells were centrifuged at 1800 rpm for 6 minutes to remove any remaining plasma. The isolated RBCs were then washed twice with phosphate-buffered saline (PBS). Various hematocrit levels from 8% to 50% were achieved by mixing the RBCs ($5x10^9$ cells/ml) with PBS. Aggregation of the RBCs was induced by using a fibrinogen mimicking macromolecule, Dextran-70 (70,000 kDa) (Sigma-Aldrich, St. Louis, MO, USA). To achieve differing degrees of aggregation, solutions of 1, 3 and 8% (wt/vol) concentration of Dextran-70 – PBS ([Dex-PBS]) were used to re-suspend NA RBCs at 40% hematocrit.

C. PA measurements

All PA measurements were conducted using the Imagio PA imaging system (Seno Medical Instruments Inc., San Antonio, TX, USA). The system consisted of a Q-switched Nd:YAG laser emitting at 1064 nm (energy 200 mJ, pulse width 6 ns, pulse repetition rate 10 Hz and beam diameter 9 mm). The ultrasound transducer mounted on the system consisted of a 4 channel annular array centered at 5 MHz (-6 dB bandwidth: 2-8 MHz) and focused at 29 mm. The RBC samples were loaded into a 14 mm cylindrical plastic sample holder. A vertical raster scan was performed with the laser emitting 4 pulses at each location within the vertical ROI covering the entire sample holder. A total of 25 PA signals were recorded for each solution exposed, corresponding to a total of 100 laser pulses.

D. Transducer calibration measurement

The transducer was driven in pulse-echo mode (all 4 channels in parallel) by the Aerotech UTA-3 US transducer analyzer (Lewiston, PA). A needle hydrophone (Precision Acoustics, Dorstet, UK) placed at the focus of the transducer received the data through an oscilloscope (Tektronix, Beaverton, OR).

E. Signal and statistical processing

All signal and statistical processing were performed in MATLAB R2010b. A Hamming window of size 14 mm was used to localize the signal from the sample holder and minimize the spectral leakage. The power spectrum for each signal was calculated using the Fast Fourier Transform algorithm and converted to a dB scale. To remove the artifacts of the system, the transducer response was subtracted from each power spectrum. Linear regression was performed over the -6 dB bandwidth of the transducer and the slope, intercept and midband fit were computed for each PA signal. The average and standard deviation of 25 calibrated power spectra was used for comparing NA with AG RBCs. A Shapiro-Wilk test for normality was performed for each PA spectral parameter from both samples ($W>0.05$). Once the normality of the data was established, an unpaired t-test was used to compare NA with AG slope, intercept and midband fit. A p-value of 0.05 or less was considered statistically significant.

III. Results And Discussion

Fig. 1 shows the variation of the average theoretical PA power spectra at various hematocrit levels for NA RBCs. The spectral power generally increased as the number of cells within the ROI (hematocrit) increased. The dominant PA frequency contained in the signals is related to the size of the individual RBCs [17], [18]. The increase in spectral power corresponds to a monotonic increase in the amplitude of the PA signals with increasing hematocrit. Other experimental measurements confirm the observed trend [19]. This increase in signal strength can be linked to the increase in the concentration of RBCs which act as PA sources.

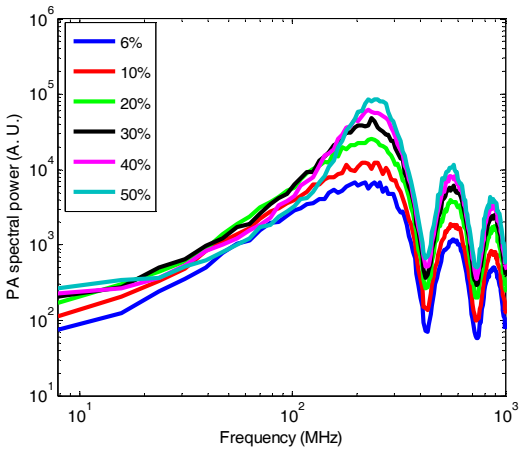

Fig. 1. Simulated average PA power spectra from NA RBCs at various hematocrit levels.

The simulated average PA power spectra for AG RBCs are shown in Fig. 2. As the size of the aggregate increases, the spectral power in the low frequency regime (< 30 MHz) increases. For example, at 15.6 MHz, a 9 dB enhancement is observed for a 10 µm RBC cluster compared to the NA case (and at the same hematocrit). The alteration of the spatial organization and size of the RBCs (NA to AG) could cause significant reduction in the destructive interference of the PA signals in the low frequency regime. The change in size causes an increase in the PA strength. This resulted in significant enhancement of the spectral power in this frequency range, which is directly linked to the aggregate size. The theoretical results suggest that NA blood samples could be distinguished from AG samples using PA RF spectroscopy.

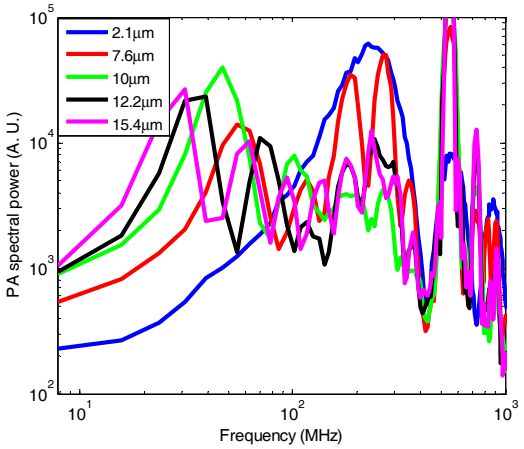

Fig. 2. Simulated average PA spectra from AG RBCs samples with aggregates of varying sizes. The aggregate size of 2.1 µm corresponds to the size of non-aggregated RBCs.

The experimental PA signal amplitudes for the NA and AG RBCs are shown in Fig. 3. As predicted by the simulations, a linear increase in signal amplitude is observed for NA RBCs. For the AG case at 40% hematocrit, the PA signal amplitude follows a non-linear behavior with increasing [Dex-PBS]. For a [Dex-PBS] of 3%, the PA amplitude is highest. This is in agreement with other experimental works which find that for the same [Dex-PBS] used, 1 and 8% show similar levels of aggregation while 3% yields the most aggregated sample [20].

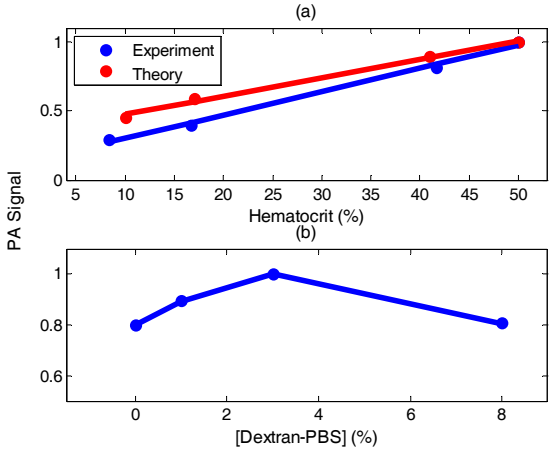

Fig. 3. Experimental PA signals for (a) NA and (b) AG RBC samples. A [Dex-PBS] of 0% corresponds to NA RBCs.

Non-calibrated, average, experimental PA power spectra for NA and the 3% [Dex-PBS] AG samples are shown in Fig. 4. Within the -6 dB bandwidth of the transducer, the AG samples show significant enhancements in spectral power compared to the NA samples. Enhancements as high as 10 dB are observed at 5 MHz (the transducer's center frequency). Since controlling the aggregate size is not possible, it is likely that spectral variations observed could arise from differing aggregate sizes. As shown by the simulation results in Fig. 2, differences as small as a few microns in the AG RBCs samples yield significant shifts in the frequency spectrum.

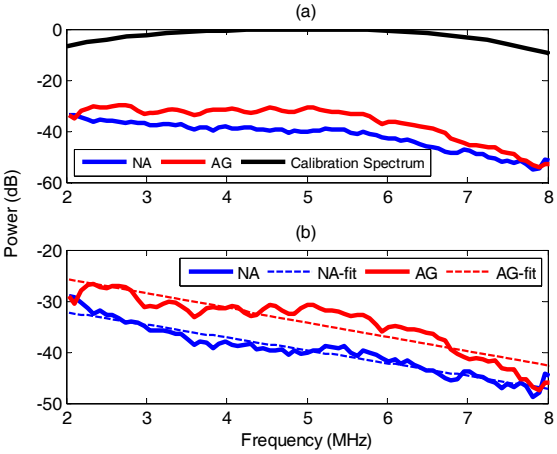

Fig. 4. Experimental, (a) non-calibrated and (b) calibrated, average PA power spectra for NA and AG RBC samples and the linear fits.

Table II shows the statistical results for the PA spectral parameters of NA and AG RBC samples. The NA sample is suspended in PBS at 40% hematocrit while the AG sample at the same hematocrit is suspended in 3% [Dex-PBS]. With the exception of the slope parameter, all other parameters are statistically significantly different. An increase is observed for all AG spectral parameters compared to the NA ones. The increase in was 0.3 dB/MHz for the slope, 3.4 dB for the intercept and 4.6 dB for the midband fit.

TABLE II
PA SPECTRAL PARAMETERS

Spectral Parameter	Slope (dB/MHz)	Intercept (dB)	Midband Fit (dB)
Non-Aggregated	-3.6 ± 0.7	-18.2 ± 5.8	-36.1 ± 2.3
Aggregated	-3.3 ± 0.3	-14.8 ± 3.2	-31.5 ± 2.4
t-test (*p* value)	0.0547	0.0135	<0.0001

It is important to note that the PA spectral parameters used here provide a potential assessment of the changes that occur during the aggregation process. They offer the opportunity to remove all the system and user dependent settings that make it difficult to compare studies under different experimental conditions. Through the frequency domain analysis of the RF signals, information about the optical properties of the sample as well as the size of the PA source could be gained [17]. Kumon et al. utilize a similar approach for distinguishing normal prostate tissue from adenocarcimona and Patterson et al. for monitoring laser heated bovine liver ex-vivo [14], [21].

However, the relationship between the PA spectral parameters to tissue properties is yet to be determined. In US tissue characterization, the spectral slope is an indicator of effective scatterer shape and size and an increase in slope corresponds to a decrease in effective scatterer size [11]. Similarly, the midband fit is a measure of the US backscatter and depends on the scatterer shape, size, acoustic impedance and concentration. As the RBCs in blood vessels are thought to be the main absorbing tissue structure responsible for the generation of US, similar spectral analysis will likely provide detail about vascular microstructure [15], [22]. Experimental RF signals could then be modeled by implementing the effects of a finite transducer bandwidth on the theoretical results presented in this work. This would give the ability to perform spectral analysis with a known concentration of PA sources and sizes thus establishing the relationship between spectral parameters and microvascular structure. Moreover, by changing the laser illumination wavelength, functional information about the oxygenation status of blood could also be obtained.

IV. Conclusion

This paper presents the first reported investigation of RBC aggregation using PA. The theoretical framework presented here elucidates the differences between NA and AG RBC samples using a frequency domain solution to PA wave propagation and spectral analysis of PA RF data. Experimental results confirm in principle the theoretical findings and suggest the potential of PA for detecting the differences between blood samples.

Acknowledgment

The financial support of NSERC, CIHR, CFI and the Canada Research Chairs Program is acknowledged. E.H. is supported through the NSERC Graduate Scholarship program. We are also thankful to Drs. Min Rui and. Sankar Narasimhan as well as Arthur Worthington and Devesh Bekah for their assistance.

References

[1] O. K. Baskurt et al. "New guidelines for hemorheological laboratory techniques," *Clin Hemorheol Micro*, vol. 42, pp. 75-97, 2009.

[2] P. C. Johnson, J. J. Bishop, S. Popel and M. Intaglietta, "Effects of red cell aggregation on the venous microcirculation," *Biorheology*, vol. 36, pp. 457-60, 1999.

[3] A. Kavitha and S. Ramakrishnan, "Assesment of human red blood cell aggregation using image processing and wavelets," *Meas Sci Rev*, vol. 7(2), pp. 43-51, 2007.

[4] H. J. Meiselman, "Red blood cell aggregation: 45 years of being curious," *Biorheology*, vol. 46, pp. 1-19, 2009.

[5] S. J. Lee, H. Ha, and K. H. Nam, "Measurement of red blood cell aggregation using X-ray phase contrast imaging," *Opt Express*, vol. 18(25), pp. 26052-61, 2010.

[6] X. Xu, L. Yu, and Z. Chen. "Velocity variation assessment of red blood cell aggregation with spectral domain Doppler optical coherence tomography," *Ann Biomed Eng*, vol. 38(10), pp. 3210-17.

[7] F. T. H.Yu and G. Cloutier, "Experimental ultrasound characterization of red blood cell aggregation using the structure factor size estimator (SFSE)," *J Acoust Soc Am*, vol. 122, 645-56, 2007.

[8] B. G. Teh and G. Cloutier, "Modeling and analysis of ultrasound backscattering by spherical aggregates and rouleaux of red blood cells," *IEEE T Ultrason Ferr*, vol. 47(4), pp. 1025-35, 2000.

[9] C. Li and L. V. Wang, "Photoacoustic tomography and sensing in biomedicine," *Phys Med Biol*, vol. 54, pp. R59-92, 2009.

[10] X. Wang, X. Xie, G. Ku, L. V. Wang and G. Stoica, "Noninvasive imaging of hemoglobin concentration and oxygenation in rat brain using high resolution photoacoustic tomography," *J Biomed Opt*, vol. 11(2), pp. 024015-1-9, 2006.

[11] F. L. Lizzi et al. "Theoretical framework for spectrum analysis in ultrasonic tissue characterization," *J Acoust Soc Am*, vol. 73(4), pp. 1366-73, 1983.

[12] M. C. Kolios and G. J. Czarnota, "Potential use of ultrasound for the detection of cell changes in cancer treatment," *Future Oncol*, vol. 5(10), pp. 1527-32, 2009.

[13] F. L. Lizzi et al. "Relationship of ultrasonic spectral parameters to features of tissue microstructure," *IEEE T Ultrason Ferr*, 33(3), pp. 319-29, 1987.

[14] R.E. Kumon, C. X. Deng and X. Wang, "Frequency-domain analysis of photoacoustic imaging data from prostate adenocarcinoma tumors in a murine model," *Ultrasound Med Biol*, vol. 37(5), pp. 834-39, 2011.

[15] J. Zalev and M. C. Kolios, "Detecting abnormal vasculature from photoacoustic signals using wavelet-packet features," *Proc SPIE*, vol. 7899, pp. 78992M-1:15, 2011.

[16] R. K. Saha and M. C. Kolios, "A simulation study on photoacoustic signals from red blood cells," *J Acoust Soc Am*, vol. 129(5), pp. 2935-43, 2011.

[17] G. J. Diebold, "Photoacoustic monopole radiation: Waves from objects with symmetry in one, two and three dimensions," in *Photoacoustic Imaging and Spectroscopy*, L. V. Wang, Ed. London: Taylor & Francis Group, 2009, pp. 3-17.

[18] M. Rui, W. Bost, E. C. Weiss, R. Lemor and M. C. Kolios, "Photoacoustic microscopy and spectroscopy of individual red blood cells," *OSA Opt & Photo Congress*, BIOMED/DH - BSuD93, 2010.

[19] A. B. Karpiouk et al., "Combined ultrasound and photoacoustic imaging to detect and stage deep vein thrombosis: phantom and *ex vivo* studies," *J Biomed Opt*, vol. 13(5), pp. 054061-1-8, 2008.

[20] O. K. Baskurt, R. A. Farley and H. J. Meiselman, "Erythrocyte aggregation tendency and cellular properties in horse, human and rat: a comperative study," *Am J Physiol Heart Circ Physiol,* vol 273, pp. H2604-12, 1997.

[21] M. P. Patterson, C. B. Riley, M. C. Kolios and W. M. Whelan, "Optoacoustic signal amplitude and frequency spectrum analysis laser heated bovine liver *ex-vivo*," *IEEE IUS*, 2011, in press.

[22] J. Zalev, "Detection and monitoring for cancer and abnormal vasculature by photoacoustic signal characterization of structural morphology," M.Sc. thesis, Ryerson Univ., 2010.